

EFFECT OF ANNEALING TEMPERATURE ON THE Li^+ IONIC CONDUCTIVITY OF $\text{La}_{0.67-x}\text{Li}_{3x}\text{TiO}_3$

LE DINH TRONG

Faculty of Physics, Hanoi Pedagogical University No. 2

PHAM DUY LONG

Institute of Materials Science, VAST

NGUYEN NANG DINH

College of Technology, Vietnam National University, Hanoi

Abstract. Perovskite $\text{La}_{0.67-x}\text{Li}_{3x}\text{TiO}_3$ with $x = 0.10, 0.11, 0.12$ and 0.13 were firstly annealed at 800°C then treated by reactive milling, followed by post-annealing at temperatures from 1100 to 1200°C . The crystalline structure of grain and grain-boundary were characterized by XRD and SEM. The impedance measurements showed that nanocrystalline $\text{La}_{0.67-x}\text{Li}_{3x}\text{TiO}_3$ after being annealed at 1150°C possessed a grain conductivity as high as $1.3 \times 10^{-3} \text{ S.cm}^{-1}$. The grain-boundary conductivity was enhanced one order in magnitude after annealing at temperature higher 1100°C and consists of $5.8 \times 10^{-5} \text{ S.cm}^{-1}$. The results have also showed the limitation of the adiabatic thermal treatment for the improvement of the grain-boundary conductivity and suggested the way to overcome the limitation by rapidly cooling the samples from the high temperature to room temperature.

I. INTRODUCTION

Superionic conductors or solid electrolytes are the subjects that have been concentrated to deal with both the theoretical and experimental researches, due to their prospective applications in many scopes, such as microelectronics, solid lithium batteries, electrochromic display [1-3]. Among these materials, much attention has been paid to lithium ion conducting perovskites (ABO_3). The first paper was reported by Belous et al. [4]. Later, Inaguma et al. have shown that a high conductivity of the perovskite lanthanum lithium titanate has been found [5]. Recently, we reported [6] on ionic conductivity of perovskite $\text{La}_{0.67-x}\text{Li}_{3x}\text{TiO}_3$ prepared by solid state solution reaction. The sample with $x = 0.11$ had the best ionic conductivity, at room temperature it was as high as $3,1 \times 10^{-5} \text{ S.cm}^{-1}$ and increased up to a value of $6 \times 10^{-3} \text{ S cm}^{-1}$ at 200°C . Though they are not suitable for solid electrolytes of lithium batteries due to the low reduction-proof against lithium metal, the fundamental studies are still important in the field of solid-state ionics and solid-state chemistry. Therefore, from perovskite-type lithium ion conductors, $\text{La}_{0.67-x}\text{Li}_{3x}\text{TiO}_3$ compounds are the most attractive due to their high conductivities, complex structures including microstructures, and have been extensively investigated concerning their structures and lithium ion conductivities. In ref. [7] the authors showed that there was a strong correlation between structure and percolative diffusion pathways in the perovskites that was primarily referred to the ordered arrangement of La ions, and

the “bottleneck” square - surrounded by four oxygen ions determined by the distortion and tilt of TiO₆ octahedral. In addition, the 90° -oriented micro-domain structure, which also influences the percolative diffusion pathways in La_{0.67-x}Li_{3x}TiO₃ was also observed. It is seen that the grain boundaries have strongly affected to the bulk ionic conductivity (i.e. total conductivity of the conductivities of the grains and grain boundaries) of the perovskite La_{0.67-x}Li_{3x}TiO₃. The way to increase the bulk ionic conductivity is to prepare samples with the grain conductivity as large as possible and to lower the grain boundaries resistance. With this aim we have made effort to synthesize samples of the La_{0.67-x}Li_{3x}TiO₃ compounds with different x-compounds of Li that was doped, consequently annealed at different temperatures. The crystalline structure, surface morphology and ionic conductivity of the samples have been studied.

II. EXPERIMENTAL

The La_{0.67-x}Li_{3x}TiO₃ solid solution samples with x = 0.10; 0.11; 0.12; and 0.13, abbreviated as M10, M11, M12 and M13, respectively were prepared from stoichiometric amounts of TiO₂ (99.99%), Li₂CO₃, (99.99%) and freshly dehydrated La₂O₃ (99.9%) purchased from Aldrich. These starting materials were grinded by a grinder of “Fritsch model Pulverisette 6”, then calcinated in platinum crucibles at 800 °C for 10 h. After grinding and pressing again, a second heating treatment - annealing was performed on smaller pellets ($\phi = 12.5$ mm, d = 1.4 mm, pressure of 500 MPa) at 1100, 1150, 1200 and 1250 °C for 4 h. The heating sweep rate is 5 °C.min⁻¹ and the cooling is natural. The crystalline structure has been studied by using X-ray diffraction analysis (XRD, Siemen D5000 diffractometer) and the surface morphology - by FE-SEM microscope (Model S4800, Hitachi). The ionic conductivity of the samples was characterized on AutoLab. Potentiostat-PGS30 using FRA-2 impedance software. To characterize impedance spectroscopy (IS) the samples were mechanically polished and chemically treated in order to have clean and parallel surfaces, then on these surfaces a metallic silver coating with 6 mm-diameter circle was vacuum evaporated. Sintered cylindrical pellets 12.5 mm in diameter and 1.4 mm in thick, with the evaporated silver electrodes, were used for electrical measurements. IS measurements were recorded under normal atmosphere between room temperature (RT) and 200 °C, in the frequency range 0.1 Hz to 1.0 MHz. The grain and grain boundaries conductivity was obtained by fitting experimental data with the theoretical curves using appropriate equivalent schema.

III. RESULTS AND DISCUSSION

III.1. Crystalline structure and morphology

From XRD analysis it has been seen that after being calcinated at 800 °C between La₂O₃, Li₂CO₃ and TiO₂ occurred solid state reaction to remove CO₂ and to form chemical bonding of La, Li, Ti and O atoms, consequently to create some compounds of La_{0.66}TiO₃, Li₂Ti₃O₇, La₂Ti₃O₇ and La(OH)₃ as shown in Fig. 1.

After thermal grinding, above mentioned structure phases have disappeared, instead a single phase structure with the compound of La_{0.67-x}Li_{3x}TiO₃ was obtained (see XRD patterns “a” for the as-grinded sample in Fig. 2). Moreover, the fact that XRD showed

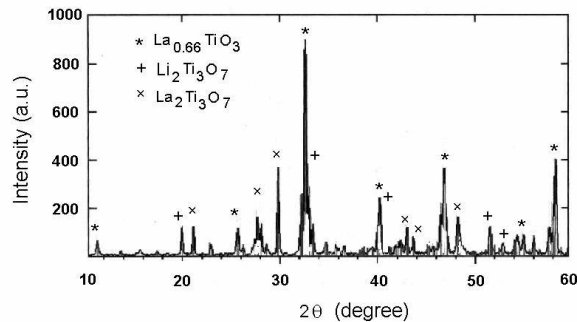


Fig. 1. XRD patterns of $\text{La}_{0.67-x}\text{Li}_{3x}\text{TiO}_3$ samples after calcination at $800\text{ }^\circ\text{C}$.

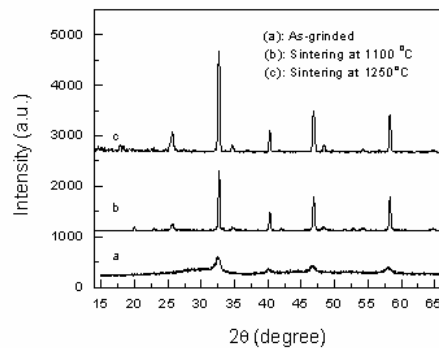


Fig. 2. XRD patterns of $\text{La}_{0.67-x}\text{Li}_{3x}\text{TiO}_3$ samples: as-grinded (pattern “a”), after annealed at $1100\text{ }^\circ\text{C}$ (pattern “b”) and at $1250\text{ }^\circ\text{C}$ (pattern “c”).

rather small and broad peaks in the 2θ range from 30° to 60° proves the uniform distribution of the nanostructured single $\text{La}_{0.67-x}\text{Li}_{3x}\text{TiO}_3$ compound. Using Sherrer’s formula one can calculate the average size of the nanostructure grains in this polycrystalline samples (it is about 30 nm).

Annealing at temperature from $1100\text{ }^\circ\text{C}$ to $1250\text{ }^\circ\text{C}$ enabled these samples be recrystallized, therefore the crystallinities increased and the nanosize grains were grown up to several micrometers (XRD patterns “b” and “c” in Fig. 2). The sample annealed at $1250\text{ }^\circ\text{C}$ exhibited larger grains size in comparison with the sample annealed at $1100\text{ }^\circ\text{C}$.

From all the XRD patterns in Fig. 2 one can see that by using reactive milling solid solution mixture from stoichiometric oxides of TiO_2 , Li_2CO_3 and La_2O_3 in combining with post-annealing, the single crystalline phase of a $\text{La}_{0.67-x}\text{Li}_{3x}\text{TiO}_3$ compound has been prepared.

The clearer picture of the grain growth can be seen by using scanning electron microscope. Figure 3 shows the FE-SEM images obtained for sample M10 which was annealed at 1100, 1150, 1200 and $1250\text{ }^\circ\text{C}$. Although a step of annealing temperature was only $50\text{ }^\circ\text{C}$, with the increase of the anneal temperature the grain size considerably

increased, from 1 μm (at 1100 °C) to 5 μm (at 1250 °C). In the sample annealed at 1100 °C there were observed large pores (Fig. 3a) and these pores were diminished by annealing at higher temperature (Figs. 3b to 3d).

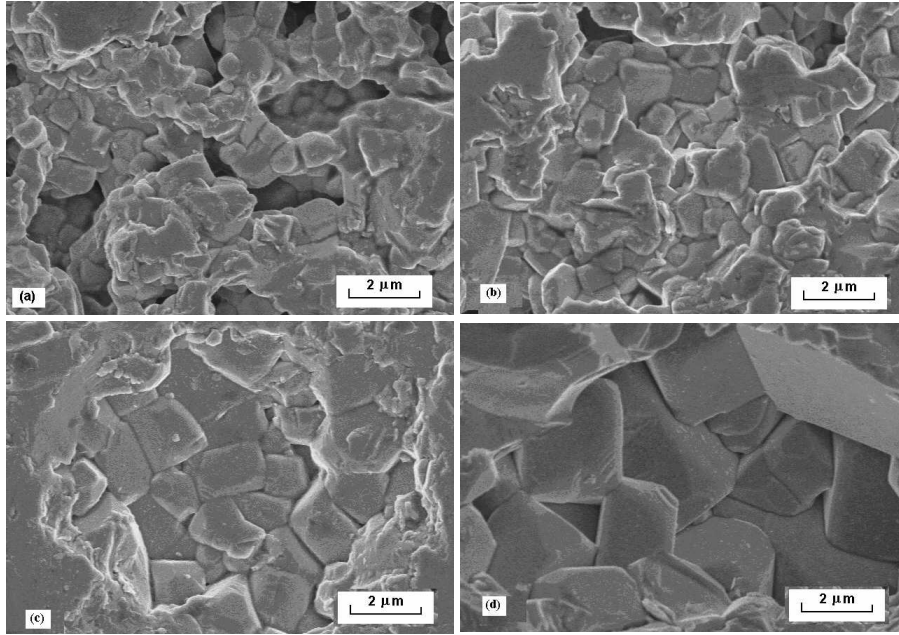


Fig. 3. FE-SEM of the sample M10 annealed at 1100 °C (a), 1150 °C (b), 1200 °C (c) and 1250 °C (d).

III.2. Ionic conductivity

For characterization of ionic conductivity it is necessary to carry-out impedance spectra measurements throughout a large range of frequencies from 0.1 Hz to 100 MHz. Due to this behavior of the grain, grain-boundary conductance and the contact resistance of the electrodes can be revealed in the complex impedance diagrams (CID) of the samples. The semicircle of impedance spectra at the higher 0.1 MHz frequencies is related to the conducting process in crystalline grains, whereas the semicircle in the CID at average frequencies (from 10 Hz to 1MHz) reflects the ionic conducting in the grain boundaries. The line starting from the end of the semicircles at the frequencies lower 10Hz is related to the diffusion process of ions in Helmholtz layer between the electrodes and the sample.

Since the semicircle of the complex impedance diagram in the high frequency range is much smaller than that in the low frequencies range, the investigation of the grain and grain-boundary ionic conductivity of the sample is carried-out and elaborated separately each from other. This is demonstrated in Fig. 4. Figures 4a and 4b correspond to high (30 MHz \div 0.3 MHz) and low (0.1 MHz \div 100 Hz) frequencies ranges, respectively for the Nyquist complex impedance diagram measured at room temperature of sample M11, that annealed at 1200 °C. The ending of the first semicircle (Fig. 4a) at about $Z' = 200 \Omega$

is the starting of the second semicircle (Fig. 4b) which has the ending at frequency of 27 Hz with a real part of the resistance of 33 kΩ. The first semicircle exhibits the behavior of ionic conductance in grains and the second one is of grain boundaries, as described in [8-9].

In almost potentiostats like the AutoLab-PGS-30 the frequency range is from 1.0 MHz to 0.01 Hz. Therefore, the first semicircle obtained in the range from 30 MHz to 300 kHz there observed several points with such a small value of resistance that was not revealed together with the high resistance values of the second semicircle. Thus grain resistance (R_g) and the total resistance (R_g+R_{gb}) of the sample can be evaluated, respectively from the right ending points of the first and the second semicircles in Fig. 4a and 4b. Qualitatively, one can compare R_{gb} and R_g by the ratio of the two ending point values in Z' abscissa from this figure. Indeed, the obtained ratio was found to be of $30\text{ k}\Omega/200\ \Omega = 1.5 \times 10^2$, this means the grain-boundary resistance is larger than the grain resistance in more than two orders in magnitude. That is why to improve the ionic conductivity is necessary to lower the grain-boundary resistance.

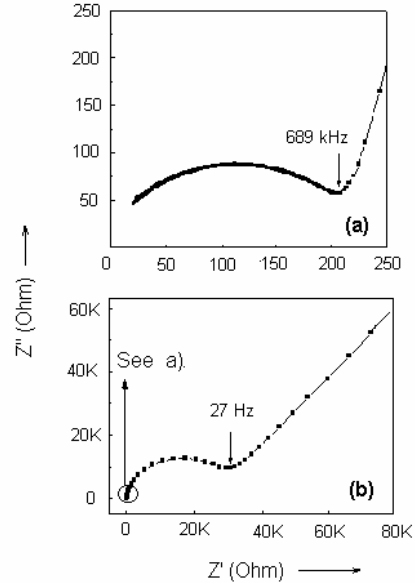


Fig. 4. Complex impedance diagrams of sample M11 annealed at 1200 °C. The measurements at room temperature and in the range of frequencies from 30 MHz to 300 kHz (a) and from 1.0 MHz – 0.1 Hz (b).

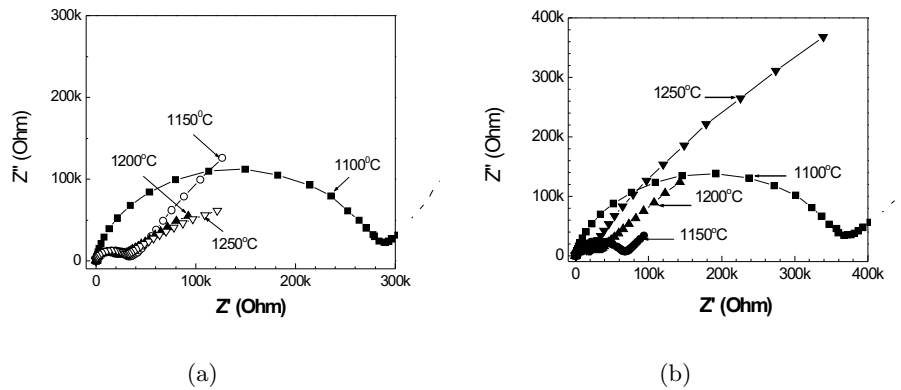


Fig. 5. Complex impedance diagrams vs. temperature of samples M10 (a), M11 (b).

Fig. 5 shows the CID of the samples M10 and M11 annealed at temperatures of 1100 °C, 1150 °C, 1200 °C and 1250 °C. All the measurements were carried-out at room temperature. From this figure one can see that all the CIDs consist of two parts: the

first part is the semicircle relating to grain-boundary conductivity and the second one is the line obtained at low frequencies that relates to the diffusion process in the Helmholtz layer. The fact that the increase of annealing temperature resulted in the diminishing of the semicircles proves that the grain-boundary conductance much decreased. This is explained by (i) with higher annealing temperature the grains were larger grown, consequently the number of grain boundaries decreased and (ii) the crystalline structure of the grains became more perfected. From the FE-SEM one can see the structure of the grains and grain boundaries were much enhanced from the annealing temperature of 1100 °C to 1200 °C.

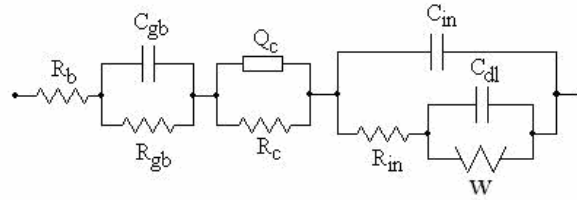


Fig. 6. Equivalent schema used for fitting the CID data of the $\text{La}_{0.67-x}\text{Li}_{3x}\text{TiO}_3$ sampes.

For the accurate determination of the ionic conductivity we used a fitting method between experimental curves and the theoretical curves obtained from equivalent schema to the CIDs. These CIDs of the $\text{La}_{0.67-x}\text{Li}_{3x}\text{TiO}_3$ samples with Ag electrode (Ag | LLTO | Ag) were well fitted by the equivalent schema of $R_g(C_{gb}R_{gb})(R_cQ_c)(C_{in}[R_{in}(C_{dl}W)]$ that is illustrated in Fig. 6. By this schema R_g is the resistance characterizing the grain conductivity; R_{gb} and C_{gb} are the resistance and capacity of grain boundaries, respectively; R_{in} and C_{in} are the resistance and the capacity formed by the contact between the Ag thin film electrode and samples surface; W and C_{dl} are, respectively the Warburg impedance characterizing the charge shift and the capacity of the double charge layer; R_c and Q_c are, respectively the resistance and the constant phase component (CPE) related to electrodes.

To determine the ionic conductivity (σ) one can use the following formula:

$$\sigma = \frac{d}{R \cdot S}$$

where d is the thickness of the sample, S – area and R – resistance relating to ionic conductance that is determined from equivalent schema.

Figure 7 presents the curves of grain conductivity, grain-boundary conductivity and also the bulk ionic conductivity of samples M10, M11, M12 and M13 vs. the annealing temperature. All the measuring data were obtained at room temperature. From these figures one can see that the grain conductivity slightly rose up with increase of the annealing temperature and did not change more with the annealing temperatures over 1150 °C. The sample M12 (annealed at 1150 °C) has the largest grain ionic conductivity, $\sigma_g = 1.3 \times 10^{-3} \text{ S.cm}^{-1}$. This value of the conductivity is fairly larger than the one of $\text{La}_{0.67-x}\text{Li}_{3x}\text{TiO}_3$ sample that was reported by Inaguma et al. ($\sigma_g = 1.0 \times 10^{-3} \text{ S.cm}^{-1}$) [8]. This was explained by the different loss of Li ions during annealing at high temperatures.

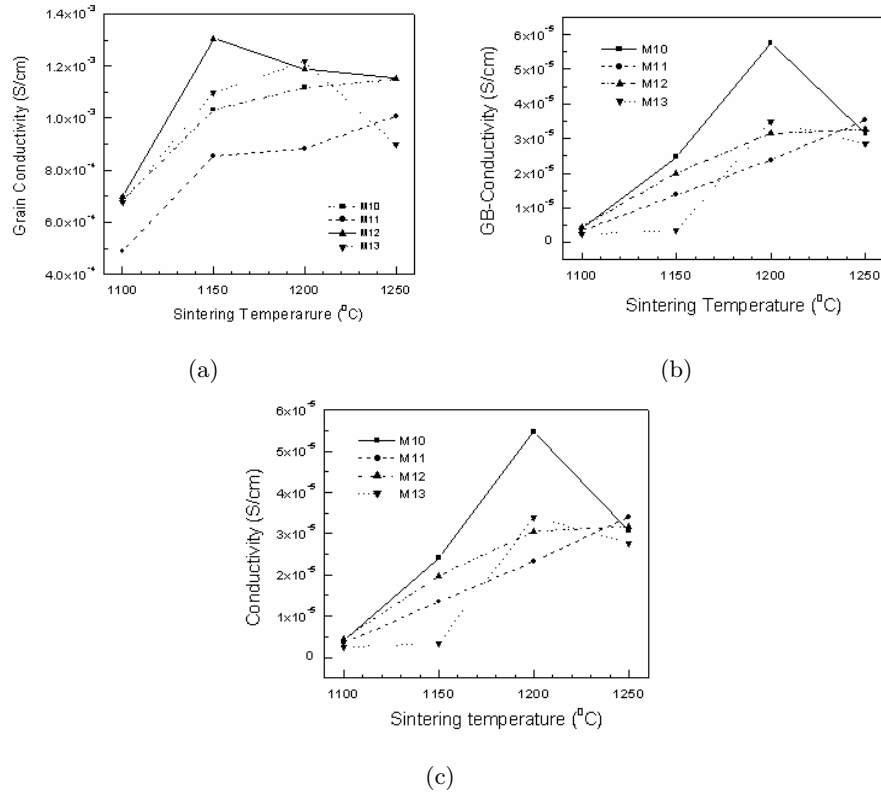


Fig. 7. The room-temperature ionic conductivity vs. annealing temperature for samples M10, M11, M12 and M13: (a) – Grain conductivity, (b) – Grain-boundaries conductivity and (c) – Bulk conductivity.

In difference with the grain conductivity, the grain-boundary conductivity increased considerably for the samples annealed at higher temperature (see Fig. 7b). It is known that this conductivity is strongly dependent on the Li-content in the boundaries, the size and the porosity of the boundaries [9]. At temperature higher 1000 °C the Li-content was maintained unchangeably, the increase in the conductivity can be attributed to the larger change in crystalline grains and boundaries. Among all the samples, the M10 which was annealed at 1200 °C exhibits the largest grain-boundary conductivity, namely $\sigma_{gb} = 5.8 \times 10^{-5} \text{ S.cm}^{-1}$. This value is one order in magnitude in comparison with the reported ionic conductivity of Ban et al. [9]. For the other samples the grain-conductivity is as low as $10^{-5} \text{ S.cm}^{-1}$ (see Fig. 7c). Although the σ_{gb} was much improved, this value is still much smaller than the σ_g (i.e. lower in two orders in magnitude). From our work, it is seen that by annealing at high temperature as we did the σ_{gb} can be increased in only one order. For enhancing bulk conductivity, the grain-boundary conductance must be more strongly lowered or a single crystal of $\text{La}_{0.67-x}\text{Li}_{3x}\text{TiO}_3$ should be grown to eliminate all grain boundaries. But the single crystal growth is unfeasible for such a complex in compounds of $\text{La}_{0.67-x}\text{Li}_{3x}\text{TiO}_3$ and for the technological difficulty. One can suggest the other effort

in enriching the Li-content of $\text{La}_{0.67-x}\text{Li}_{3x}\text{TiO}_3$ the grain boundaries by a rapid cooling technique to quenching the samples from a high temperature to RT. The detain results of this method will be reported in our forthcoming work.

IV. CONCLUSION

$\text{La}_{2/3-x}\text{Li}_{3x}\text{TiO}_3$ with $x = 0.10, 0.11, 0.12$ and 0.13 were prepared by reactive milling solid mixture from stoichiometric amounts of TiO_2 (99.99%), Li_2CO_3 , (99.99%) and La_2O_3 (99.9%), followed by post-annealing at temperature from 1100 to 1200 °C. The intergrain and intragrain conductivities were evaluated by overall analyzing the XRD patterns, FE-SEM surface morphology and impedance spectra. Because of the formation of nanocrystalline stoichiometric $\text{La}_{0.67-x}\text{Li}_{3x}\text{TiO}_3$, after being annealed at 1150 °C, the samples exhibited a grain conductivity as high as $1.3 \times 10^{-3} \text{ S.cm}^{-1}$. The grain-boundary conductivity was enhanced in one order in magnitude after annealing at temperature higher 1100 °C and consists of $5.8 \times 10^{-5} \text{ S.cm}^{-1}$. The improvement in the grain-boundaries conductivity was explained due to the decrease of the boundary effect.

The result also showed the limitation of the adiabatic annealing, consequently suggest the way to improve the bulk ionic conductivity by a rapid cooling technique for the samples from the high temperature to room temperature.

ACKNOWLEDGEMENT

This work is supported in part by Vietnam National Foundation for Basic Scientific Research in Physics (2006-2008), Project code: 410306.

REFERENCES

- [1] C. M. Lampert and C. G. Granqvist, eds, in “*Large-area Chromogenics: Materials and Devices for Transmittance Control*”, Vol. 154 (SPIE Optical Engineering Press, Bellingham, 1990)
- [2] Inaguma Y., Chen L., Itoh M., Nakamura T., Uchida T., Ikuta M., and M. Wakihara, *Solid State Commun.* **86** (1993) 689 - 693.
- [3] Y. Inaguma, L. Chen, M. Itoh, T. Nakamura, *Solid State Ionics*, **70/71** (1994) 196-202.
- [4] A. G. Belous, G. N. Novitskaya, S. V. Polyanetskaya, Yu. I. Gornikov, *Izv. Akad. Nauk SSSR, Neorg. Mater.* **23** (1987) 470-476.
- [5] Y. Inaguma, M. Itoh, *Solid State Ionics* **86–88** (1996) 257-260
- [6] N. N. Dinh, P. D. Long, L. D. Trong, *Comm. in Phys.* **14** (2004) 90-96.
- [7] Y. Inaguma, T. Katsumata, M. Itoh, Y. Morii, T. Tsurui, *Solid State Ionics* **177** (2006) 3037-3044.
- [8] C. H. Chen, K. Amine, *Solid State Ionics* **144** (2001) 51-57.
- [9] C. W. Ban, G. M. Choi, *Solid State Ionics* **140** (2001) 285–292.

Received 15 November 2008.